Characterization of the natural measure by unstable periodic orbits in nonhyperbolic chaotic systems

Ying-Cheng Lai*
Department of Physics and Astronomy and Department of Mathematics, The University of Kansas, Lawrence, Kansas 66045
(Received 11 July 1997; revised manuscript received 25 August 1997)

The natural measure of a chaotic set in a phase-space region can be related to the dynamical properties of all unstable periodic orbits embedded in part of the chaotic set contained in that region. This result has been rigorously shown to be valid for hyperbolic chaotic systems. Chaotic sets encountered in most physical situations, however, are typically nonhyperbolic. The purpose of this paper is to test the goodness of the unstable periodic-orbit characterization of the natural measure for nonhyperbolic chaotic systems. We first directly compare the natural measure from a typical trajectory on the chaotic set with that evaluated from unstable periodic orbits embedded in the set. As an indirect check, we then compute the difference between the long-time average values of physical quantities evaluated with respect to a typical trajectory and those computed from unstable periodic orbits. Results with the Hénon map for which periodic orbits can be enumerated lend credence to the conjecture that the unstable periodic-orbit theory of the natural measure is applicable to nonhyperbolic chaotic systems. [S1063-651X(97)02012-6]

PACS number(s): 05.45.+b

I. INTRODUCTION

An important problem in the study of chaotic systems is to compute long-term statistics such as averages of physical quantities, Lyapunov exponents, dimensions, and other invariants of the probability density or the measure. The interest in the statistics lies in the fact that trajectories of deterministic chaotic systems are apparently random and ergodic. These statistical quantities, however, are *physically meaningful* only when the measure being considered is the one generated by a typical trajectory in phase space. This measure is called the natural measure [1] and it is invariant under the evolution of the dynamics. Therefore, it is of paramount physical importance to be able to understand and to be able to characterize the natural measure [2] in terms of fundamental dynamical quantities. There is nothing more fundamental than to express the natural measure in terms of the periodic orbits embedded in a chaotic attractor.

A key contribution along these lines was made in Ref. [3], in which Grebogi, Ott, and Yorke obtained an expression for the invariant natural measure in terms of the magnitude of the eigenvalues of the unstable periodic orbits embedded in the chaotic attractor. They proved [3] the correctness of their expression, but only for the special case of an hyperbolic dynamics [4]. The validity of their results for physical situations, which are typically nonhyperbolic, remained, however, only a conjecture. The purpose of this paper is to provide evidence for the applicability of the results of Ref. [3] to nonhyperbolic chaotic systems and hence to validate their conjecture.

To begin, we review some fundamental properties of a chaotic system. Due to ergodicity, trajectories on a chaotic set exhibit a sensitive dependence on initial conditions. Moreover, the long-time probability distribution generated by a typical trajectory on the chaotic set is generally highly singular. Take a chaotic attractor, for example. A trajectory originated from a random initial condition in the basin of attraction visits different parts of the attractor with drastically different probabilities. Call regions with high probabilities ''hot'' spots and regions with low probabilities ''cold'' spots. Such hot and cold spots in the attractor can in general be interwoven on arbitrarily fine scales. In this sense, chaotic attractors are said to possess a multifractal structure. Due to this singular behavior, one utilizes the concept of natural measure to characterize chaotic attractors [1]. To obtain the natural measure, one covers the chaotic attractor with a grid of cells and examines the frequency with which a typical trajectory visits these cells in the limit that both the length of the trajectory goes to infinity and the size of the grid goes to zero [5]. Except for an initial condition set of Lebesgue measure zero in the basin of attraction, these frequencies in the cells are the natural measure. Specifically, let $f(\mathbf{x}_0,T,\epsilon_i)$ be the amount of time that a trajectory from a random initial condition $\mathbf{x}_0$ in the basin of attraction spends in the ith covering cell C_i of edge length ϵ_i in a time T. The probability measure of the attractor in the cell C_i is

$$\mu_i = \lim_{\epsilon_i \to 0} \lim_{T \to \infty} \frac{f(\mathbf{x}_0,T,\epsilon_i)}{T}. \tag{1}$$

The measure is called *natural* if it is the same for all randomly chosen initial conditions, that is, for all initial conditions in the basin of attraction except for a set of Lebesgue measure zero. The spectrum of an infinite number of fractal dimensions quantifies the behavior of the natural measure [6].

As a physical example, we consider a forced damped pendulum

$$\frac{dx}{dt} = y, \tag{2}$$

*Electronic address: lai@poincare.math.ukans.edu

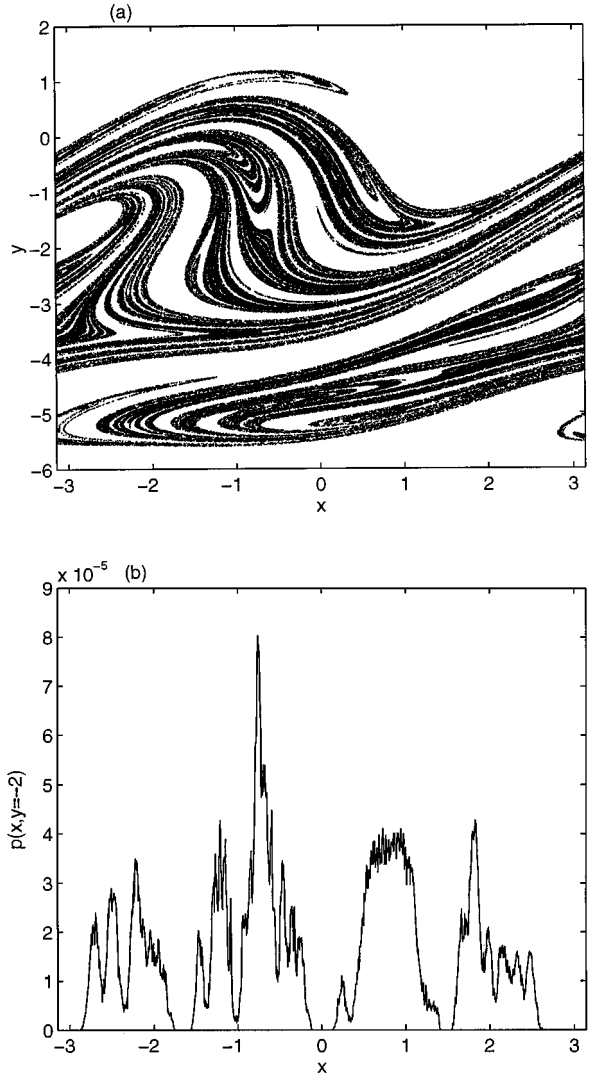

FIG. 1. For the forced damped pendulum system (2), (a) a trajectory of 1.5×10^5 points on the chaotic attractor on the stroboscopic surface of section and (b) the distribution of the natural measure in a one-dimensional array of 1000 rectangular cells in the x direction at $y=2$. The size of each cell is $2\pi/1000\times0.06$. Numerically, the total measure contained in the attractor is normalized to unity. Apparently, the natural measure is singular.

$$\frac{dy}{dt}=-0.05y-\sin x+2.5\sin t.$$

Figure 1(a) shows, on the stroboscopic surface of section defined at discrete times $t_n=2\pi n$, $n=1,...$, a trajectory of 1.5×10^5 points on the chaotic attractor, where the abscissa and the ordinate are the angle $x(t_n)$ and the angular velocity $y(t_n)\equiv dx/dt|_{t_n}$ of the pendulum, respectively. Figure 1(b) shows the one-dimensional probability distribution on the attractor at $y=-2$. To obtain Fig. 1(b), we define a one-dimensional array of 1000 rectangular cells in the x direction at $y=-2$. The size of each cell is $2\pi/1000\times0.06$. We then compute, from a trajectory of 10^7 points on the surface of section (after a sufficiently long initial transient), the frequencies of visit of the trajectory to each cell. In fact, probability distributions on any line intersecting the chaotic attractor exhibit a similar behavior. These results suggest a highly singular probability distribution on the chaotic attractor.

It is known that a chaotic attractor has embedded within itself an infinite number of unstable periodic orbits. These periodic orbits are *atypical* in the sense that they form a Lebesgue measure zero set. With probability one, randomly chosen initial conditions do not yield trajectories that exist on unstable periodic orbits. Invariant measures produced by unstable periodic orbits are thus atypical and there are an infinite number of such atypical invariant measures embedded in a chaotic attractor. The hot and cold spots are a reflection of these atypical measures. The natural measure, on the other hand, is typical in the sense that it is generated by a trajectory originated from any one of the randomly chosen initial conditions in the basin of attraction. A typical trajectory visits a fixed neighborhood of any one of the periodic orbits from time to time. Thus chaos can be considered as being organized with respect to the unstable periodic orbits [7]. An interesting question is then how the natural measure is related to the infinite number of atypical invariant measures embedded in the attractor.

In 1988, Grebogi, Ott, and Yorke addressed this fundamental question in Ref. [3], in which they derived, for the special case of hyperbolic chaotic systems [4], a formula relating the natural measure of the chaotic set in the phase space to the expanding eigenvalues of all the periodic orbits embedded in the set. Specifically, consider an N-dimensional map $\mathbf{M}(\mathbf{x})$. Let $\mathbf{x}_{ip}$ be the ith fixed point of the p-times-iterated map, i.e., $\mathbf{M}^p(\mathbf{x}_{ip})=\mathbf{x}_{ip}$. Thus each $\mathbf{x}_{ip}$ is on a periodic orbit whose period is either p or a factor of p. The natural measure of a chaotic attractor in a phase-space region S is given by

$$\mu(S)=\lim_{p\to\infty}\sum_{\mathbf{x}_{ip}\in S}\frac{1}{L_1(\mathbf{x}_{ip},p)}, \tag{3}$$

where $L_1(\mathbf{x}_{ip},p)$ is the magnitude of the expanding eigenvalue of the Jacobian matrix $\mathbf{DM}^p(\mathbf{x}_{ip})$ and the summation is taken over all fixed points of $\mathbf{M}^p(\mathbf{x})$ in S. The derivation of this formula was done under the assumption that the phase space can be divided into cells via a Markov partition, a condition that is generally satisfied in hyperbolic chaotic systems. Explicit verification of this formula was done for several analyzable hyperbolic maps [3]. Equation (3) is theoretically significant and interesting because it provides a fundamental link between the natural measure and various atypical invariant measures embedded in a chaotic attractor.

In this paper we present evidence for the validity of Eq. (3) for nonhyperbolic chaotic sets. We take two approaches: (i) *a direct check*, to compare the natural measure computed from a typical trajectory with that computed from unstable periodic orbits according to Eq. (3), and (ii) *an indirect check*, to compare the average physical quantities computed from a typical trajectory with those computed from the periodic orbits. Results with the Hénon map for which periodic orbits can be enumerated lend credence to the conjecture that the unstable periodic-orbit theory of the natural measure is applicable to nonhyperbolic chaotic systems. A short account of this work has been discussed recently [8].

The rest of the paper is organized as follows. In Sec. II we describe the rigorous derivation of Eq. (3) for hyperbolic

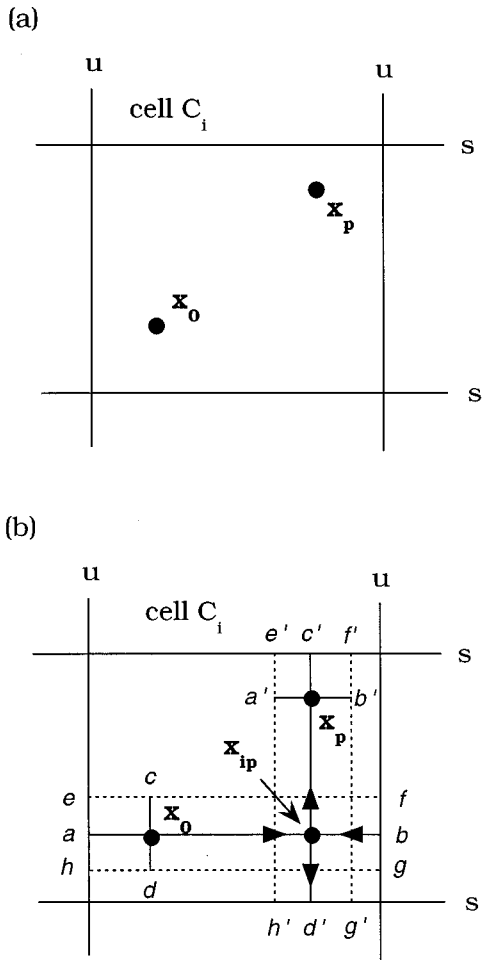

FIG. 2. (a) Initial condition $\mathbf{x}_0$ in the cell C_i and the point $\mathbf{x}_p$ that returns to C_i after p iterations. (b) Rectangle $efgh$ maps to rectangle $e'f'g'h'$ after p iterations. There must then be a fixed point $\mathbf{x}_{ip}$ of the p-times-iterated map in C_i.

chaotic systems [3]. In Sec. III we lay out our approaches to verify Eq. (3) for nonhyperbolic chaotic systems. In Sec. IV we test Eq. (3) for nonhyperbolic chaotic attractors. In Sec. V we provide evidence for the validity of Eq. (3) for nonhyperbolic chaotic saddles. In Sec. VI we present a discussion.

II. UNSTABLE PERIODIC-ORBIT THEORY OF THE NATURAL MEASURE FOR HYPERBOLIC CHAOTIC SYSTEMS

To obtain Eq. (3) [3], we first cover the chaotic set with a grid of partitioning cells, each being confined by segments of the stable and unstable manifolds. If the cells are small compared to the size of the phase-space region in which the chaotic set lies, each cell can be regarded as being rectangular, as shown in Fig. 2(a), where the horizontal and vertical sides are segments of the stable and unstable manifolds, respectively. Denote this cell by C_i. Now imagine that we choose a large number of initial conditions according to the natural measure. The natural measure contained in the cell C_i is the fraction of trajectories that return to C_i in the limit where the number of iterations $n\rightarrow\infty$. Let $\mathbf{x}_0$ be an initial condition in the cell C_i, as shown in Fig. 2(a). Due to recurrence or ergodicity, the trajectory from $\mathbf{x}_0$ returns to some point $\mathbf{x}_p$ in C_i, say, after p iterations, as shown in Fig. 2(a). Let ab be the horizontal line segment through $\mathbf{x}_0$ ending at the two unstable-manifold segments and $c'd'$ be the vertical line segment through $\mathbf{x}_p$ ending at the two stable-manifold segments, as shown in Fig. 2(b). Since ab is parallel to the stable-manifold segments and since $\mathbf{x}_0$ maps to $\mathbf{x}_p$ after p iterations, the image of ab under the p-times-iterated map $\mathbf{M}^p(\mathbf{x})$ is a shorter horizontal line segment $a'b'$ straddling $\mathbf{x}_p$. Similarly, the pth preimage of $c'd'$ is a shorter vertical line segment cd straddling $\mathbf{x}_0$. Now construct two rectangles $efgh$ and $e'f'g'h'$ with side lengths (ab,cd) and $(a'b',c'd')$, respectively, as shown in Fig. 2(b). We see that the rectangle $efgh$ maps to the rectangle $e'f'g'h'$ under $\mathbf{M}^p(\mathbf{x})$. Since both rectangles have a common overlapping region and since the dynamics is contracting in the horizontal direction and expanding in the vertical direction, there must be at least one point in the overlapping region whose location is not influenced by the action of the pth-iterated map $\mathbf{M}^p(\mathbf{x})$. That is, there must be an unstable fixed point $\mathbf{x}_{ip}$ of $\mathbf{M}^p(\mathbf{x})$ in the overlapping region in cell C_i.

To estimate the contribution to the natural measure from the fixed point $\mathbf{x}_{ip}$, we assume that $c'd'$ has a length ϵ. Thus we have $\epsilon/L_1(\mathbf{x}_{ip})$ for the length of cd, where $L_1(\mathbf{x}_{ip})$ is the unstable (expanding) eigenvalue of the fixed point $\mathbf{x}_{ip}$. Since the natural measure is uniform along the unstable direction, we see that associated with the unstable fixed point $\mathbf{x}_{ip}$, the fraction of trajectories that returns to C_i in p iterations is

$$[\epsilon/L_1(\mathbf{x}_{ip})]/\epsilon = 1/L_1(\mathbf{x}_{ip}).$$

Taking into consideration all the unstable fixed points contained in C_i and taking the limit $p\rightarrow\infty$, we obtain Eq. (3).

The above argument applies to situations where a good partition of the phase space exists such that the shorter line segments $a'b'$ and cd in Fig. 2(b) are completely contained in the cell C_i. For hyperbolic systems, such a partition exists, which is the Markov partition [9]. Therefore, Eq. (3) is rigorously valid for hyperbolic dynamical systems [3]. The argument becomes problematic for nonhyperbolic systems. A grid of cells in which each cell C_i looks like the cell in Fig. 2 cannot be constructed because of the set of an infinite number of tangency points between the stable and unstable manifolds [4]. Due to this difficulty, it is not clear whether a rigorous argument can be constructed for nonhyperbolic chaotic sets in a similar way. Therefore, the applicability of Eq. (3) to nonhyperbolic chaotic systems remains only a conjecture.

III. NUMERICAL METHODS

We study two-dimensional invertible maps, which in principle can be obtained from a system of three-dimensional ordinary differential equations through a Poincaré surface of section. A possible way to test the applicability of Eq. (3) to nonhyperbolic chaotic systems is by systematic and extensive numerical computation. Specifically, we perform the following two tests.

(i) Direct check. We cover the chaotic set with a fine grid of cells and compute the natural measure μ_i in each nonempty cell C_i according to Eq. (1). We then compute the measure $\mu_i(p)$ that is due to *all* the fixed points of the

p-times-iterated map contained in each cell C_i according to Eq. (3). Let

$$\Delta\mu(p)\equiv\sqrt{\sum_{i=1}^{N}[\mu_i(p)-\mu_i]^2/N}, \tag{4}$$

where N is the number of cells C_i with nonzero natural measure. We find that $\Delta\mu(p)$ decreases exponentially as the period p increases,

$$\Delta\mu(p)\sim\exp(-\alpha p), \tag{5}$$

where $\alpha>0$ is the scaling exponent. Equation (5) indicates that the natural measure computed from the periodic orbits approaches exponentially the one computed from a typical trajectory, thereby validating Eq. (3).

(ii) Indirect check. We compare the average values of physical quantities with respect to the natural measure evaluated from typical trajectories and those evaluated from the unstable periodic orbits. Consider a smooth scalar function $F(x,y)$ that represents some physical quantity of interest. Let $\langle F\rangle$ be the average value of $F(x,y)$ evaluated with respect to the natural measure given by Eq. (1) and let $\langle F\rangle(p)$ be the same function evaluated from the approximation of the natural measure in terms of all fixed points of the p-times-iterated map as given by Eq. (3). For a typical trajectory $\{x_n,y_n\}_{n=0}^{\infty}$ on the chaotic set, $\langle F\rangle$ can be computed using the time average and ergodicity of the chaotic set

$$\langle F\rangle=\int F(x,y)d\mu=\lim_{N\to\infty}\frac{1}{N}\sum_{n=1}^{N}F(x_n,y_n), \tag{6}$$

whereas $\langle F\rangle(p)$ is computed via

$$\langle F\rangle(p)=\sum_{j=1}^{N(p)}\mu_j(p)\left[\frac{1}{p}\sum_{i=1}^{p}F(x_{ji},y_{ji})\right], \tag{7}$$

where (x_{ji},y_{ji}) $(i=1,\ldots,p)$ are the jth fixed points of the p-times-iterated map and $N(p)$ is the total number of the fixed points of the p-times-iterated map, which scales with p as

$$N(p)\sim e^{h_T p}. \tag{8}$$

The scaling exponent h_T is the topological entropy of the chaotic set. We find again that for both nonhyperbolic chaotic attractors and nonhyperbolic chaotic saddles the difference $\Delta F(p)\equiv|\langle F\rangle(p)-\langle F\rangle|$ decreases exponentially as the period p increases:

$$\Delta F(p)\sim\exp(-\alpha p), \tag{9}$$

thereby furnishing further credance to the conjecture that Eq. (3) applies to nonhyperbolic chaotic systems as well.

From Eq. (3), we see that if S is a phase-space region that contains the entire chaotic set, we have

$$\mu(S)=\lim_{p\to\infty}\sum_{i=1}^{N(p)}\frac{1}{L_1(\mathbf{x}_{ip},p)}=1.$$

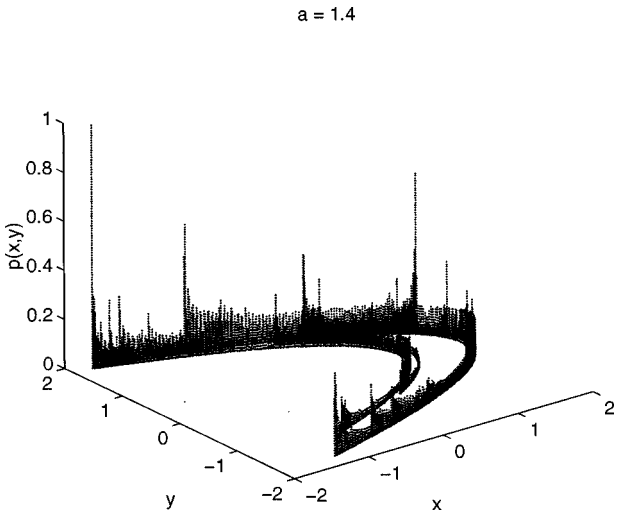

FIG. 3. Distribution of the natural measure on the Hénon attractor, where a grid of 128×128 cells is used to cover the region $(-2\leqslant x\leqslant-2,\ -2\leqslant y\leqslant2)$ in which the attractor lies and a trajectory of length 10^7 from a random initial condition is used to compute the natural measure contained in each cell.

For finite but large period p, the quantity $\Sigma_{i=1}^{N(p)}[1/L_1(\mathbf{x}_{ip},p)]$ is close to unity, but it is not exactly equal to unity. Thus we use the following rescaled value for $\mu_j(p)$ in Eq. (7):

$$\mu_j(p)=\frac{1/L_1(\mathbf{x}_{jp},p)}{\sum_{i=1}^{N(p)}1/L_1(\mathbf{x}_{ip},p)},\quad j=1,\ldots,N(p). \tag{10}$$

IV. NONHYPERBOLIC CHAOTIC ATTRACTORS

In order to be able to test the applicability of Eq. (3) to nonhyperbolic chaotic systems, it is necessary to choose a model for which *all* unstable periodic orbits of up to reasonably high periods can be computed numerically. We choose the Hénon map [10]

$$x_{n+1}=a-x_n^2+by_n,\quad y_{n+1}=x_n. \tag{11}$$

We study $a=1.4$ and $b=0.3$, a parameter setting for which the map apparently possesses a chaotic attractor. The attractor is apparently nonhyperbolic because a rigorous computation of the stable and unstable manifolds [11] points towards the existence of an infinite number of tangency points of these manifolds on the attractor. Figure 3 shows the distribution of the natural measure on the attractor, where a grid of 128×128 cells is used to cover the region $(-2\leqslant x\leqslant-2,\ -2\leqslant y\leqslant2)$ in which the attractor lies and a trajectory of length 10^7 from a random initial condition is used to compute the natural measure contained in each cell. The quantity μ_i in Eq. (4) in each nonempty cell C_i is approximately the fraction of time that the trajectory visits the cell. The distribution of μ_i is apparently singular.

The Hénon map is one of the very few model systems for which there is a numerical algorithm to compute, in principle, all unstable periodic orbits of arbitrarily high periods [12]. We have computed all the periodic orbits up to period 30. Figure 4(a) shows the locations of all 4498 periodic or-

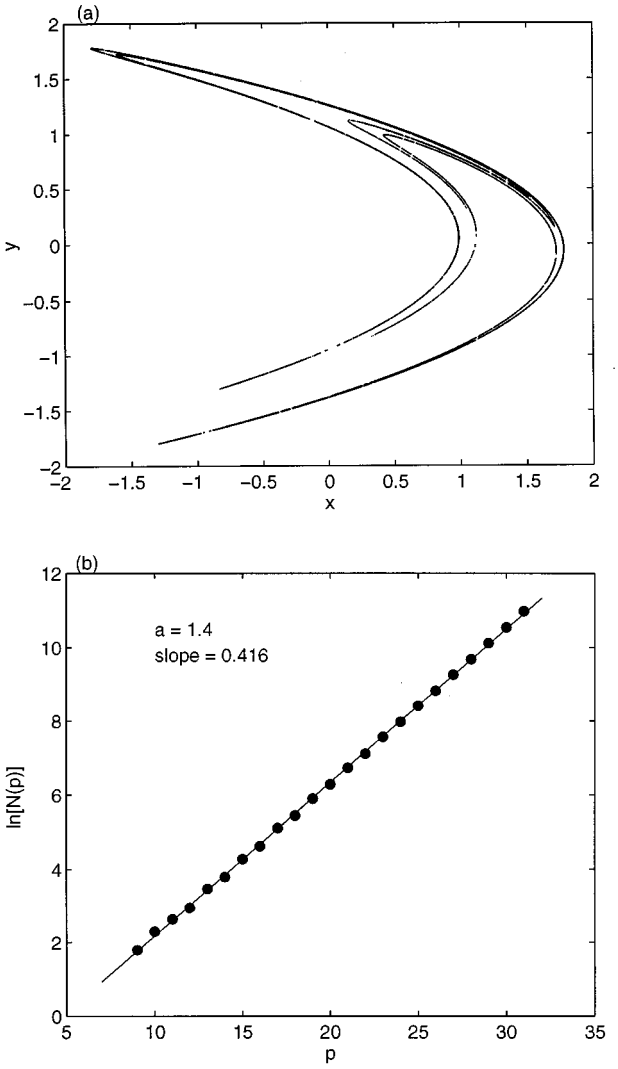

FIG. 4. (a) Locations of all 4498 periodic orbits of period 25 embedded in the Hénon attractor. (b) $N(p)$, the number of periodic orbits of period p, versus p for $9 \leqslant p \leqslant 30$ on a logarithmic scale. The slope of the fitted straight line is approximately the topological entropy h_T of the attractor, which is $h_T = 0.416 \pm 0.003$.

bits of period 25. The plot resembles that of the attractor itself, indicating that the periodic orbits are apparently dense on the attractor. Figure 4(b) shows $N(p)$ versus p for $9 \leqslant p \leqslant 30$ on a logarithmic scale, the slope of which is approximately the topological entropy h_T of the attractor. The plot gives $h_T = 0.416 \pm 0.003$.

A. Direct check

When a 128×128 grid of cells is used to cover the region $-2 \leqslant (x,y) \leqslant 2$ in Fig. 3, we find that there are 909 nonempty cells that a trajectory of 10^7 iterations on the chaotic attractor visits. We then compute, in each nonempty cell, all the fixed points $\mathbf{x}_{ip}$ of the p-times-iterated map and their associated expanding eigenvalues $L_1(\mathbf{x}_{ip}, p)$ to obtain the quantity $\mu_i(p)$ in Eq. (4). Figure 5(a) shows $\ln \Delta\mu(p)$ versus p for $6 \leqslant p \leqslant 30$. We observe the scaling relation (5), where $\alpha \approx 0.14$ is the scaling exponent. Thus we see that the quantitative characterization of the natural measure of the chaotic attractor by unstable periodic orbits becomes exponentially

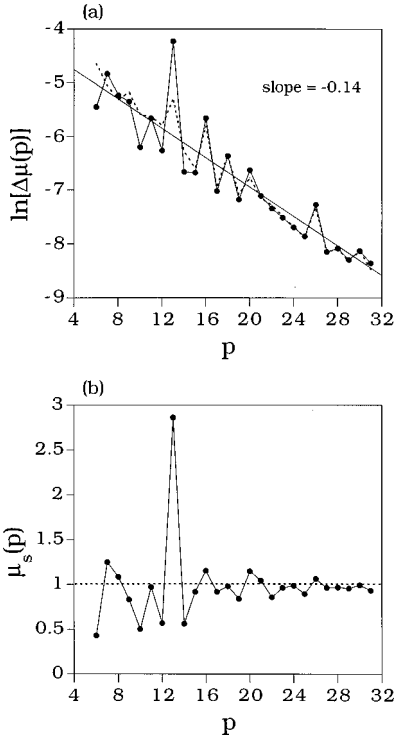

FIG. 5. For the Hénon chaotic attractor, (a) $\ln \Delta\mu(p)$ versus p. We have, approximately, $\Delta\mu(p) \sim e^{-0.14p}$. (b) Total period-$p$ natural measure $\mu_S(p)$ computed from Eq. (3) using all the period-p orbits. The total measure approaches to unity as p increases. The dashed line in (a) is $\ln \Delta\mu(p)$ versus p, but the quantity $\mu_i(p)$ is rescaled by $\mu_S(p)$.

accurate as the period p increases. Asymptotically, we have $\Delta\mu(p) \to 0$, indicating the applicability of Eq. (3) to nonhyperbolic chaotic sets. It is interesting to note that the somewhat large fluctuations in Fig. 5(a) is partly due to the fact that there are fewer periodic orbits of lower period p, since their number increases with p exponentially, where the exponential rate is the topological entropy. Figure 5(b) shows the period-p natural measure of the entire attractor $\mu_S(p) \equiv \sum_{i=1}^{N(p)} \mu_i(p)$ versus p. It can be seen that $\mu_S(p)$ approaches unity rapidly as p increases. The dashed line in Fig. 5(a) is $\ln \Delta\mu(p)$ versus p, but the quantity $\mu_i(p)$ is rescaled by $\mu_S(p)$, as in Eq. (10). The rescaled plot has a slope similar to the unscaled one (the solid line), but the fluctuations are smaller. We find that Eq. (5) appears to hold regardless of the fineness of the grid used to cover the attractor. For instance, plots almost identical to those in Fig. 5(a) are obtained when grids 64×64 and 256×256 are used. Thus we expect Eq. (3) to be valid for any phase-space region containing part of the chaotic set in nonhyperbolic systems.

To understand the *exponential* scaling law (5), we utilize a simple one-dimensional analyzable model: the doubling transformation $x_{n+1} = 2x_n \bmod (1)$. All periodic orbits of period p of this map have the same eigenvalue 2^p. Divide the unit interval into N bins so that the size of each bin is $\epsilon = 1/N$. The natural measure contained in each bin is ϵ because it is uniform in the unit interval. There are $(2^p \pm 1)/N$ fixed points of the pth-fold map in each bin so that $\mu_i(p) = [(2^p \pm 1)/N]/2^p = \epsilon(1 \pm 2^{-p})$. Thus we have $\Delta\mu(p) = |\mu_i(p) - \epsilon| \sim 2^{-p} = \exp(-p \ln 2)$. Notice that the

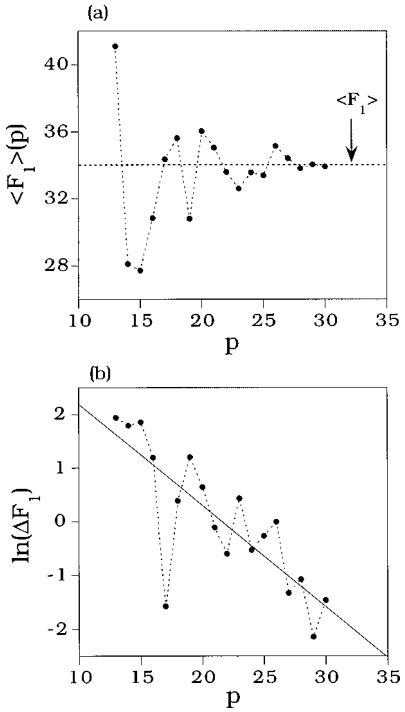

FIG. 6. (a) Average value $\langle F_1\rangle(p)$ of the physical function $F_1(x,y)=\exp(x^2+y^2)$ computed from all periodic orbits of period p. As the period p increases, $\langle F_1\rangle(p)$ asymptotically approaches $\langle F_1\rangle$, the average value computed from a typical trajectory. (b) $\Delta F_1(p)\equiv|\langle F_1\rangle(p)-\langle F_1\rangle|$ versus p on a semilogarithmic scale. The plot suggests the scaling relation (9).

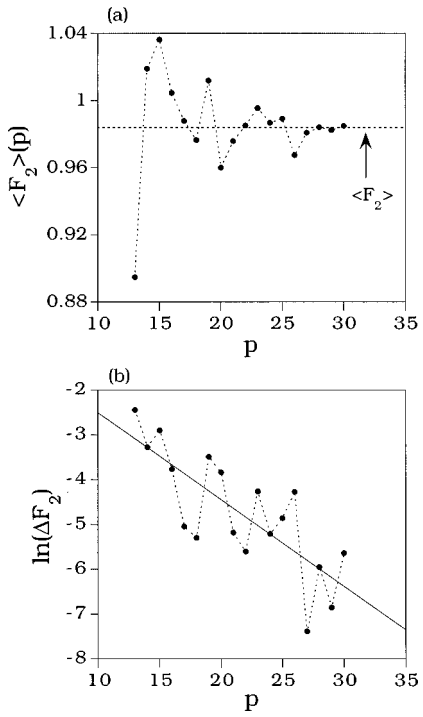

FIG. 7. (a) Average value $\langle F_2\rangle(p)$ of the physical function $F_2(x,y)=\cos(\pi/4)(x+y)+\sin(\pi/4)(x+y)$ computed from all periodic orbits of period p. As the period p increases, $\langle F_2\rangle(p)$ approaches rapidly $\langle F_2\rangle$. (b) $\Delta F_2(p)\equiv|\langle F_2\rangle(p)-\langle F_2\rangle|$ versus p on a semilogarithmic scale. The plot suggests the same scaling relation (9) with a similar scaling exponent to that in Fig. 6(b).

scaling exponent for the doubling transformation is ln2, which is the topological entropy. This is due to the fact that the natural measure is uniform and all periodic-orbit points have the same eigenvalue. For more complicated nonhyperbolic systems, such as the one in our numerical example, the natural measure is highly nonuniform and the positive Lyapunov exponents of all the period-p orbits are not the same but obey some probability distribution with width proportional to $\sqrt{p}$ [13]. Thus the scaling exponent in Eq. (5) is less than the topological entropy. We have also checked the scaling (5) for another hyperbolic map, the Kaplan-Yorke map [14], and have found that the exponent is approximately the topological entropy. It is thus interesting to note that nonhyperbolicity makes the scaling exponent deviate from the topological entropy, but nonetheless the scaling law is still exponential.

B. Indirect check

For concreteness, we choose the following two smooth functions (rather arbitrarily) for a numerical test:

$$F_1(x,y)=\exp(x^2+y^2),$$

$$F_2(x,y)=\cos\frac{\pi}{4}(x+y)+\sin\frac{\pi}{4}(x+y). \tag{12}$$

To compute $\langle F_1\rangle$ and $\langle F_2\rangle$ we use 10^6 trajectories, each having a length of 500 and resulting from a random initial condition in the region $-0.5\leqslant(x,y)\leqslant 0.5$. The first 500 iterations are discarded for each trajectory. We obtain $\langle F_1\rangle=34.135\pm0.005$ and $\langle F_2\rangle\approx0.981\pm0.001$. Figure 6(a) shows $\langle F_1\rangle(p)$ versus p. It can be seen that $\langle F_1\rangle(p)$ rapidly converges to $\langle F_1\rangle$ as p increases. Figure 6(b) shows $\Delta F_1(p)\equiv|\langle F_1\rangle(p)-\langle F_1\rangle|$ versus p on a semilogarithmic scale. The plot can be fit roughly by a straight line, indicating the scaling relation (9), where the scaling exponent α is the slope of the fit, which is approximately -0.19 ± 0.07. Figures 7(a) and 7(b) show the same computation for $F_2(x,y)$, where now the scaling exponent is approximately -0.19 ± 0.08. We note that there are large fluctuations in Figs. 6(b) and 7(b), resulting in large uncertainties in the estimation of the slopes. This is because we compute orbits only up to period 30. There is in principle no difficulty in computing periodic orbits of higher periods, but the task has become practically infeasible at present. Despite uncertainties in the slopes, we see that Eq. (9) approximately holds for both $F_1(x,y)$ and $F_2(x,y)$ with scaling exponents similar to that in Eq. (5). These results thus suggest that Eq. (9) holds regardless of the details of the physical function, thereby providing additional support for Eq. (3) for nonhyperbolic chaotic attractors.

V. NONHYPERBOLIC CHAOTIC SADDLES

We now consider nonhyperbolic chaotic saddles. For the Hénon map at $b=0.3$, a crisis occurs at $a_c\approx1.426$, after which the chaotic attractor becomes a nonattracting chaotic saddle [15]. Figure 8(a) shows a trajectory of 1.5×10^5 points

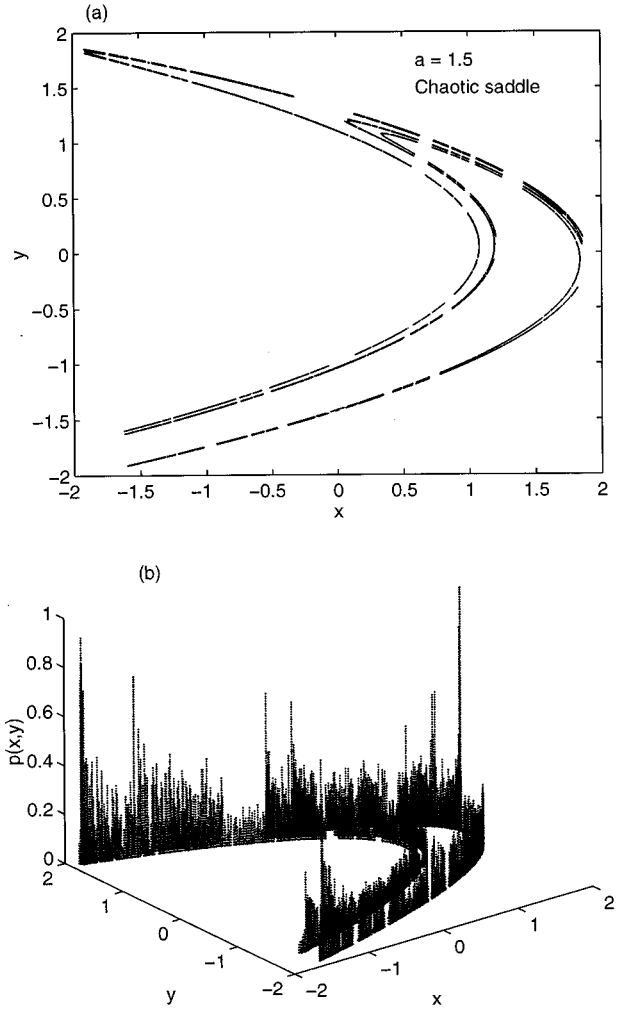

FIG. 8. (a) Trajectory of 1.5×10^5 points for the chaotic saddle at $a=1.5$ of the Hénon map. (b) Highly singular distribution of the natural measure on the chaotic saddle.

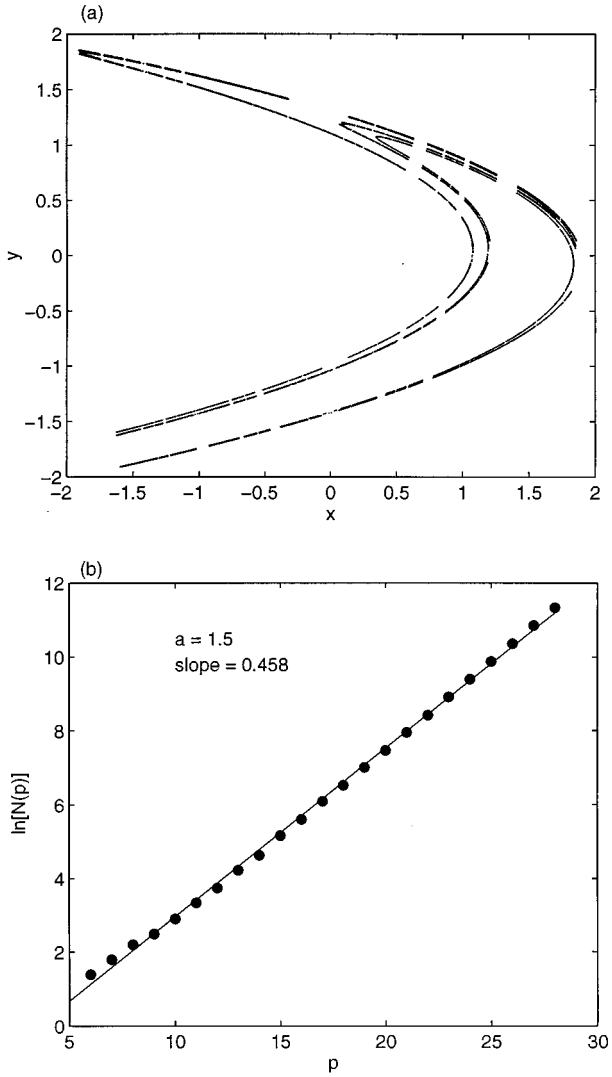

FIG. 9. (a) Locations of all 4566 periodic orbits of period 22 embedded in the chaotic saddle in Fig. 8(a). (b) $\ln N(p)$ versus p, from which we obtain the topological entropy of the chaotic saddle: $h_T=0.458\pm0.008$.

the chaotic saddle for $a=1.5$. The trajectory is computed by using the PIM-triple method (where PIM denotes proper interior maximum) that is particularly designed for finding continuous trajectories on chaotic saddles in two-dimensional maps [16]. Computation of angles between the stable and unstable directions reveals that the angle can be arbitrarily close to zero, suggesting that the chaotic saddle in Fig. 8(a) is nonhyperbolic [17]. Figure 8(b) shows the distribution of the natural measure on the chaotic saddle, where a grid of 128×128 cells is used to cover the region $-2\leqslant(x,y)\leqslant2$ in which the chaotic saddle lies and 1000 trajectories on the saddle, each having length 10^4, are used to compute the natural measure contained in each cell. The natural measure is apparently highly singular. To verify Eq. (3), we compute the periodic orbits embedded in the chaotic saddle for periods up to 28. We did not go to higher periods due to computer limitation, as the topological entropy of the chaotic saddle is larger than that of the chaotic attractor at $a=1.4$. Figure 9(a) shows the locations of all 4566 periodic orbits of period 22. A comparison between Figs. 9(a) and 8(a) suggests that these periodic orbits appear to be dense on the chaotic saddle. Figure 9(b) shows $\ln N(p)$ versus p, from which the topological entropy of the chaotic saddle is estimated to be $h_T=0.458\pm0.008$.

For nonattracting chaotic saddles, the natural measure about the jth periodic orbit of period p needs to be modified to $e^{p/\tau}/L_j$, where τ is the average lifetime of an ensemble of trajectories staying in some phase-space region containing the chaotic saddle [3]. But this modification does not affect the rescaled natural measure defined in Eq. (10). Figures 10(a) and 10(b) show $\ln\Delta F_1(p)$ and $\ln\Delta F_2(p)$ versus p, respectively, where the asymptotic values $\langle F_1\rangle$ and $\langle F_2\rangle$ are computed by using 10^4 PIM-triple trajectories on the chaotic saddle, each having length 1000 with 1000 preiterations. The plots can be roughly fit by straight lines, the slopes of which are -0.21 ± 0.05 and -0.23 ± 0.07 for Figs. 10(a) and 10(b), respectively. Thus we see that the periodic-orbit characterization of the natural measure seems to hold for nonhyperbolic chaotic saddles as well.

VI. DISCUSSION

In summary, we have presented evidence for the validity of the theory that relates the natural measure to unstable

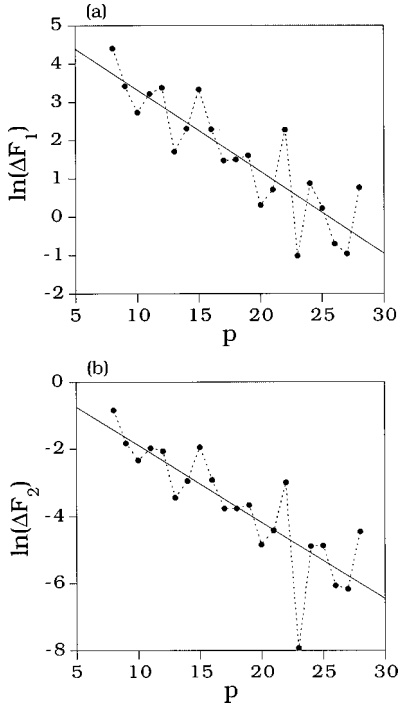

FIG. 10. (a) $\ln\Delta F_1(p)$ and (b) $\ln\Delta F_2(p)$ versus p for the chaotic saddle in Fig. 8(a). Both plots suggest the scaling relation (9).

periodic orbits for nonhyperbolic chaotic attractors and chaotic saddles. Our conclusion is that such a theory, while previously shown to be valid for hyperbolic systems [3], is apparently correct for nonhyperbolic chaotic systems too. Unstable periodic orbits play a pivotal role in determining the dynamics on chaotic sets. These orbits are the fundamental building blocks of chaotic sets since they support the natural measure, apparently even for nonhyperbolic sets as indicated by our numerical investigations herein. Dynamical invariants such as the Lyapunov exponents, topological entropy, and even the spectrum of fractal dimensions of a chaotic set, hyperbolic or not, can now be determined based on the natural measures expressed in terms of the unstable periodic orbits embedded in the set. The periodic-orbit theory is conceptually appealing and is potentially useful for further theoretical or even practical developments [18,19].

In order to characterize the natural measure by unstable periodic orbits, it is necessary to compute the locations of all periodic orbits up to reasonably high periods, which is in general a difficult task *even for discrete maps*. However, we believe that our results for nonhyperbolic chaotic systems are general because our numerical example, the Hénon map, has been a paradigm in the study of chaotic systems.

We stress in this paper that although the periodic-orbit theory of the natural measure was confirmed numerically by utilizing exclusively discrete maps, we expect the theory to be valid for continuous chaotic systems as well. Our confidence relies on the well-known fact that the dynamics of a continuous flow can be faithfully represented by that of a discrete map on a Poincaré surface of section [20]. It has then become possible for Eq. (3) to be tested because certain discrete maps (not many of them, though) allow for the computation of *all* periodic orbits up to some reasonably high periods. As such, our numerical results can be regarded as an *indirect* check for the periodic-orbit characterization of the natural measure for continuous dynamical systems. It would certainly be interesting to be able to check the applicability of our theory for continuous systems directly, but this demands a direct computation of *all* unstable periodic orbits up to high periods for continuous flows. While certain periodic orbits can be computed for continuous flows such as the Lorenz system [21], at present we are not aware of any numerical procedure that allows for a *systematic* computation of all periodic orbits from a continuous system.

ACKNOWLEDGMENTS

I thank Professor Celso Grebogi for valuable discussions and Y. Nagai for assisting in the numerical computation. This work was sponsored by AFOSR under Grant No. F49620-96-1-0066, by NSF under Grants Nos. DMS-962659 and PHY-9722156, and by the University of Kansas.

[1] R. Bowen and D. Ruelle, Invent. Math. **79**, 181 (1975).

[2] In fact, physicists in statistical mechanics and ergodic theory expend great effort in the characterization of invariant measures.

[3] C. Grebogi, E. Ott, and J. A. Yorke, Phys. Rev. A **37**, 1711 (1988).

[4] The dynamics is hyperbolic on a chaotic set if at each point of the trajectory the phase space can be split into an expanding and a contracting subspace and the angle between them is bounded away from zero. Furthermore, the expanding subspace evolves into the expanding one along the trajectory and the same is true for the contracting subspace. Otherwise the set is nonhyperbolic. In general, nonhyperbolicity is a complicating feature because it can cause fundamental difficulties in the study of the chaotic systems, a known one being the shadowability of numerical trajectories by true trajectories [C. Grebogi, S. M. Hammel, and J. A. Yorke, J. Complexity **3**, 136 (1987); Bull. Am. Math. Soc. **19**, 465 (1988); C. Grebogi, S. M. Hammel, J. A. Yorke, and T. Sauer, Phys. Rev. Lett. **65**, 1527 (1990); S. Dawson, C. Grebogi, T. Sauer, and J. A. Yorke, *ibid.* **73**, 1927 (1994)].

[5] J. D. Farmer, E. Ott, and J. A. Yorke, Physica D **7**, 153 (1983).

[6] P. Grassberger, Phys. Lett. **97A**, 227 (1983); H. G. E. Hentschel and I. Procaccia, Physica D **8**, 435 (1983); P. Grassberger, Phys. Lett. **107A**, 101 (1985); T. C. Halsey, M. J. Jensen, L. P. Kadanoff, I. Procaccia, and B. I. Shraiman, Phys. Rev. A **33**, 1141 (1986).

[7] G. H. Gunaratne and I. Procaccia, Phys. Rev. Lett. **59**, 1377 (1987); D. Auerbach, P. Cvitanović, J.-P. Eckmann, G. H. Gunaratne, and I. Procaccia, *ibid.* **58**, 2387 (1988); D. Auerbach, B. O'Shaughnessy, and I. Procaccia, Phys. Rev. A **37**, 2234 (1988); P. Cvitanović and B. Eckhardt, Phys. Rev. Lett. **63**, 823 (1989); D. Auerbach, Phys. Rev. A **41**, 6692 (1990).

[8] Y.-C. Lai, Y. Nagai, and C. Grebogi, Phys. Rev. Lett. **79**, 649 (1997).

[9] R. Bowen, *On Axiom A Diffeomorphisms*, CBMS Regional Conference Series in Mathematics (American Mathematical Society, Providence, 1978), Vol. 35.
[10] M. Hénon, Commun. Math. Phys. **50**, 69 (1976).
[11] Z. You, E. J. Kostelich, and J. A. Yorke, Int. J. Bifurcation Chaos **1**, 605 (1991).
[12] O. Biham and W. Wenzel, Phys. Rev. Lett. **63**, 819 (1989); Phys. Rev. A **42**, 4639 (1990).
[13] R. S. Ellis, *Entropy, Large Deviations and Statistical Mechanics* (Springer-Verlag, New York, 1985).
[14] J. L. Kaplan and J. A. Yorke, in *Functional Differential Equations and Approximations of Fixed Points*, edited by H.-O. Peitgen and H.-O. Walter, Lecture Notes in Mathematics Vol. 730 (Springer, Berlin, 1979), p. 204.
[15] C. Grebogi, E. Ott, and J. A. Yorke, Phys. Rev. Lett. **48**, 1507 (1982); Physica D **7**, 181 (1983).
[16] H. E. Nusse and J. A. Yorke, Physica D **36**, 137 (1989).
[17] Y.-C. Lai, C. Grebogi, J. A. Yorke, and I. Kan, Nonlinearity **6**, 779 (1993).
[18] Chaos **2** (1) (1992), special issue on periodic orbit theory, edited by P. Cvitanović.
[19] A. Katok, Publ. Math. IHES **51**, 377 (1980); T. Morita, H. Hata, H. Mori, T. Horita, and K. Tomita, Prog. Theor. Phys. **78**, 511 (1987); D. P. Lathrop and E. J. Kostelich, Phys. Rev. A **40**, 4028 (1989); D. Pierson and F. Moss, Phys. Rev. Lett. **75**, 2124 (1995); D. Christini and J. J. Collins, *ibid.* **75**, 2782 (1995); X. Pei and F. Moss, Nature (London) **379**, 619 (1996); B. Hunt and E. Ott, Phys. Rev. Lett. **76**, 2254 (1996); P. So, E. Ott, S. J. Schiff, D. T. Kaplan, T. Sauer, and C. Grebogi, *ibid.* **76**, 4705 (1996); P. So, E. Ott, T. Sauer, B. J. Gluckman, C. Grebogi, and S. J. Schiff, Phys. Rev. E **55**, 5398 (1997); P. Schmelcher and F. K. Diakonos, Phys. Rev. Lett. **78**, 4733 (1997).
[20] See, for example, K. T. Alligood, T. Sauer, and J. A. Yorke, *Chaos: An Introduction to Dynamical Systems* (Springer, New York, 1996).
[21] S. M. Zoldi and H. S. Greenside (unpublished).